2.4 Advances in Metal-Carbene Chemistry

Department of Organometallic Chemistry by Alois Fürstner

ABSTRACT: The major lines of research in this Department continue to be: (i) alkyne metathesis, (ii) iron catalyzed C-C-bond formation, (iii) π-acid catalysis using platinum, gold and rhodium complexes, and (iv) unorthodox catalytic addition reactions. All areas are prospering, including the application of the in-house methodology to target-oriented synthesis; yet, it was the field of ruthenium-catalyzed addition chemistry which led to the most perplexing and (hopefully) significant results. For the unexpected intervention of discrete metal carbenes as reactive intermediates, the major findings in this area are discussed together with our recent contributions to the related field of rhodium carbene chemistry.

Ruthenium. *cis*-Delivery of H_2 to a π-system of an unsaturated substrate is the canonical course of metal catalyzed hydrogenation reactions. This stereochemical paradigm remained basically unchallenged since the pioneering work of Sabatier until our group reported the semi-reduction of internal alkynes with the aid of [Cp*Ru]-based catalysts. The reaction clearly violates this fundamental rule and affords *E*-alkenes by direct *trans*-hydrogenation (Scheme 1). Answering the question as to how this unorthodox transformation might proceed and whether it is a singularity or the manifestation of a more general reactivity mode became a top priority in our laboratory.[1]

Scheme 1. Prototypical *trans*-Hydrogenation Reaction

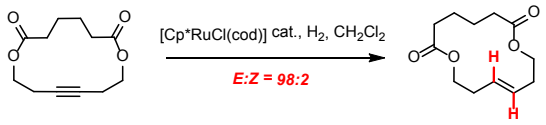

A combined experimental and theoretical approach provided compelling evidence that *trans*-hydrogenation can actually be reached by *two* distinctly different yet interconnected pathways (Scheme 2).[2] A σ-complex of type **A** is initially formed, which evolves via the rate-determining H-delivery to the activated triple bond into a metallacyclopropene **B**. It is at this stage that the reaction pathway bifurcates: thus, **B** can transform in a concerted process into the desired *E*-alkene **E** by passing through a low-lying stereo-determining transition state; this product-forming step is strongly exergonic and therefore almost certainly irreversible. The computed barrier for the formation of the Z-alkene is notably higher, which explains the experimentally observed excellent *E*/*Z* ratios.

Reagents other than H_2 able to form σ-complexes similar to **A** should undergo analogous *trans*-addition to alkynes. In fact, we were able to accomplish closely related *trans*-hydroboration, *trans*-hydrosilylation (previously described by the Trost laboratory), *trans*-hydrogermylation and *trans*-hydrostannation reactions, which are equally paradigm-changing processes.[1] The stereochemical outcome is astounding, if one considers that conventional *trans*-hydroboration is *the* textbook example for a *cis*-addition process via a four-membered transition state under frontier-orbital control. All newly discovered *trans*-hydrometalation reactions break this fundamental stereochemical rule; importantly, they are robust, distinguished by excellent functional group compatibility, and have already stood the test of natural product synthesis in a number of demanding cases (see below).[1]

Scheme 2. Mechanism of *trans*- and *gem*-Hydrogenation

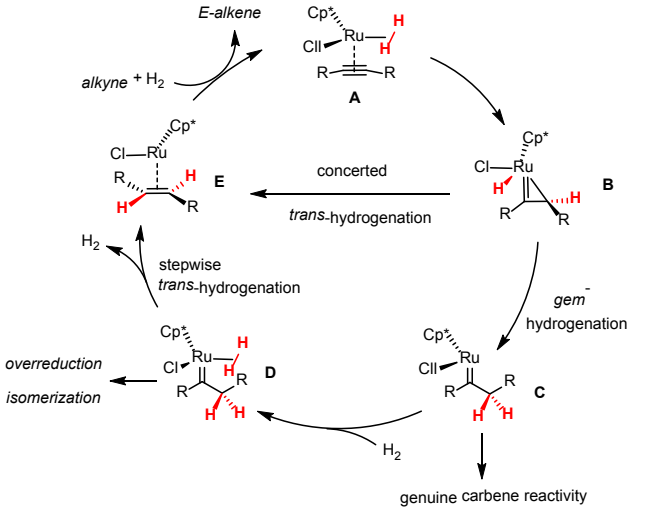

Only in the case of the *trans*-hydrogenation can the metallacyclopropene **B** evolve by a second pathway, in which both H-atoms of H_2 are transferred to one and the same C-atom of the substrate (Scheme 2). This geminal delivery, which entails formation of a discrete metal carbene **C**, is without precedent in the literature. Computational studies at the DFT and the CCSD(T)) level suggest that the *trans*- and the *gem*-pathway have similar barriers, but polar substituents in vicinity to the reacting triple bond foster carbene formation and allow regioselectivity to be imposed on this remarkable transformation (Figure 1). Moreover, it has been unambiguously shown by spectroscopic means (PHIP NMR) that the

resulting carbenes are kinetically competent intermediates rather than thermodynamic sinks off the catalytic cycle; they evolve via associative H_2-dependent processes into the desired *E*-alkene (and possible by-products). The spectroscopic evidence is in excellent accord with the computational results.[2]

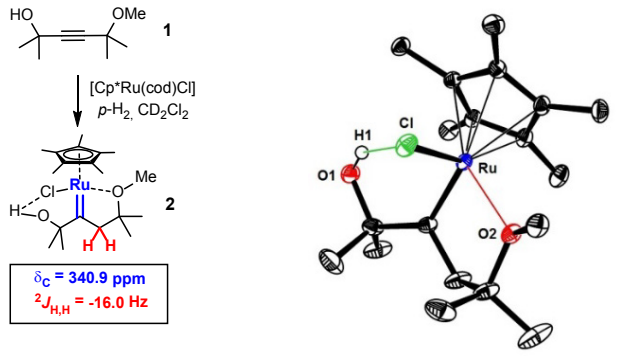

Figure 1. Formation of a Pianostool Ru-Carbene by *gem*-Hydrogenation; Structure of the Complex in the Solid State

Scheme 3. Hydrogenative Cyclopropanation and Hydrogenative Metathesis

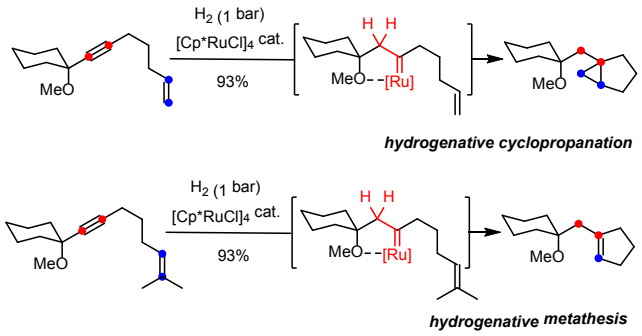

From a conceptual viewpoint, the formation of discrete metal carbenes by hydrogenation of an alkyne is arguably of the highest significance. In a formal sense, the triple bond behaves as a 1,2-dicarbene synthon: one "carbene" intercepts the [Cp*Ru] fragment, whereas the vicinal "carbene" site inserts into the H–H bond (Figure 1). To the best of our knowledge, the *geminal* hydrogenation of a stable carbogenic compound is a new reactivity mode.[1,2]

This counterintuitive entry into ruthenium carbenes raises new questions and opens exciting chemical opportunities. Even though we were able to isolate and even crystallize numerous examples, it is not intuitive whether such pianostool ruthenium complexes exhibit Fischer-carbene or Schrock-alkylidene character. For two representative complexes, however, has it been possible to record the solid-state ^{13}C NMR spectra and to analyze the chemical shift tensors of the carbene signals.[3] Details apart, this advanced spectroscopic technique drew the portrait of a family of metal carbenes that amalgamates purely electrophilic behavior with characteristics more befitting metathesis-active Grubbs catalysts. Moreover, we were able to show that less electron-rich Cp^R ligands facilitate carbene formation by *gem*-hydrogenation.[3]

Several attempts at harnessing genuine carbene reactivity by alkyne *gem*-hydrogenation have already been successful.[2] Most notably, it is possible to intercept the carbene primarily formed with tethered olefins (Scheme 3); this allows either cyclopropenes or cyclic olefins to be formed; it is the substitution pattern of the substrate that determines the course of the reaction.[4] In any case, the new "hydrogenative cyclopropanation" stands in striking contrast to the hydrogenolytic cleavage of cyclopropanes commonly used in organic synthesis. Likewise, the "hydrogenative metathesis" is an entirely new manifold to be distinguished from classical enyne metathesis, because it delivers cyclic olefins rather than 1,3-dienes as the product. The available data allow a fairly detailed mechanistic picture to be drawn, especially with regard to the fate of the secondary carbene formed during the actual metathetic C–C bond cleavage.[4]

***trans*-Hydrometalation**. As mentioned above, the concerted pathway of *trans*-hydrogenation (**A** → **B** → **E**) finds correspondence in ruthenium catalyzed *trans*-additions of pinacolborane (pinBH) or R_3EH (E = Si, Ge, Sn) to internal alkynes.[1] During the report period, these reactions were subject to extensive scrutiny. They are distinguished by excellent stereo- as well as regioselectivity, especially when working with propargylic substrates:[5] spectroscopic, crystallographic and computational evidence suggests that a nascent hydrogen bond between the protic substituent and the polarized [Ru–Cl] unit of the catalyst locks the substrate in place; at the same time, the –Cl ligand steers the incoming reagent via a hypervalent interaction with the R_3E– group (Scheme 4). These synergistic effects impose directionality on the ligand sphere of the loaded catalyst **F**, which ultimately translates into excellent levels of selectivity.[5]

Scheme 4. Directed *trans*-Hydrometalation and Novel Downstream Chemistry

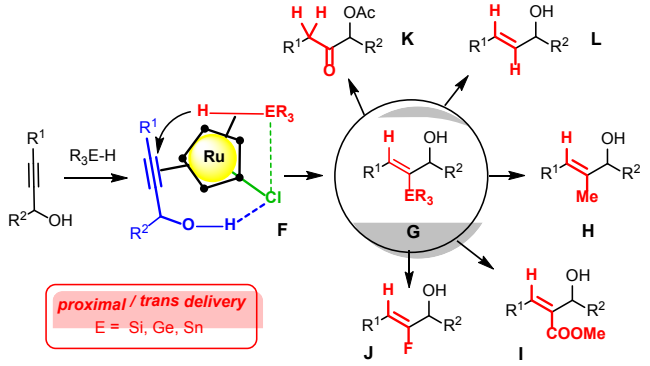

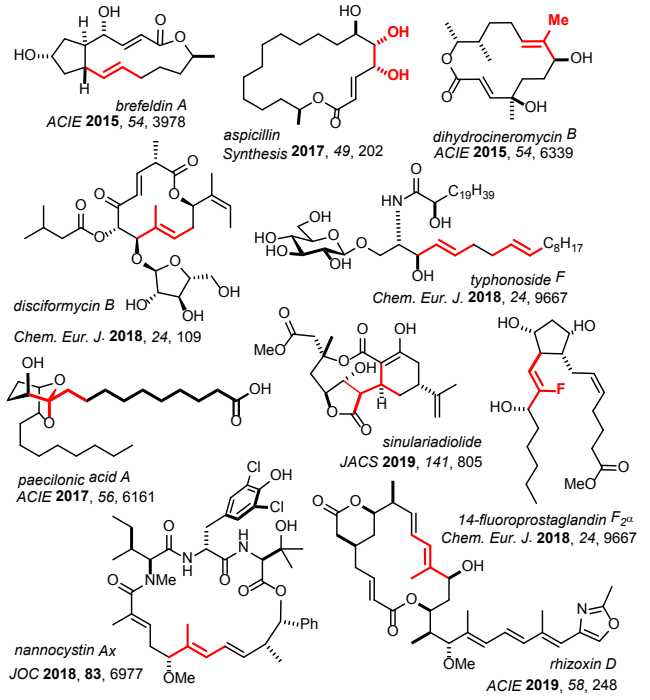

The resulting products **G** provide ample opportunity for downstream functionalization. In addition to the known repertoire of organoboron, -silicon and –tin chemistry, we developed new methods that allow such substrates to be converted into the polyketide motifs **H** and **I** by C-methylation or methoxycarbonylation, respectively. Likewise, stereodefined fluoroalkenes **J** as well as acyloins **K** came into reach (Scheme 4). Each of these transformations has already served as a key step in natural product synthesis.

Scheme 5. Total Synthesis of Sinulariadiolide

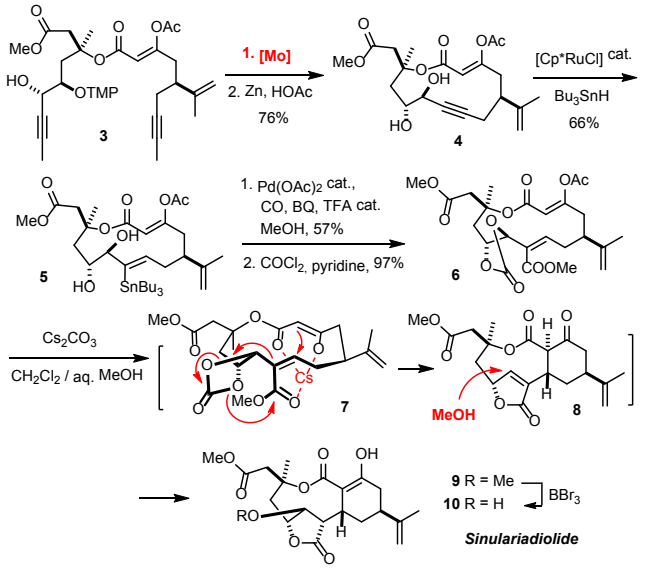

The arguably most involved case concerns the *nor*-cembranoid sinulariadiolide (**10**) (Scheme 5).[6] Specifically, a transannular approach was conceived, which allowed the tricyclic scaffold comprising a central nine-membered ring to be forged. Key to success was the formation of the macrocyclic precursor **4** by alkyne metathesis (this laboratory) followed by hydroxy-directed *trans*-hydrostannation (this laboratory) and subsequent methoxycarbonylation of the resulting stannane **5** (this laboratory). Treatment of compound **6** thus formed with Cs_2CO_3 in MeOH triggered a cascade comprised of (i) deacetylation, (ii) stereoselective transannular Michael addition with formation of the challenging medium-sized ring, (iii) β-elimination with concomitant cleavage of the carbonate, (iv) attack of the released alkoxide onto the proximal ester with formation of a butenolide ring **8**, and (iv) front-side attack of MeOH from the medium onto this Michael acceptor, which is rendered particularly reactive by the bridgehead alkene moiety. Final ether cleavage then furnished the target compound in excellent overall yield.[6]

Rhodium. Controlled decomposition of diazo compounds with (chiral) dirhodium tetracarboxylate complexes has gained tremendous importance in (asymmetric) catalysis. The transient rhodium carbenes, however, had basically defied direct experimental observation until our group was able in 2016 to present crystal structures of several prototypical members of this elusive series (cf. last progress report). NMR data showed that the structures in solution are very similar to those in the solid state.

The crystal structure of the donor-acceptor carbene **11** derived from $[Rh_2((S)\text{-PTTL})_4]$ (**12**), a chiral catalyst with an excellent track record, is deemed particularly relevant (Figure 2).[7] Although crystallographic and spectroscopic data can only draw the portrait of the ground state, it is likely that the forces which impose the peculiar and – at first sight – unexpected "all-up" conformation onto the chiral ligand sphere are also operative in the selectivity-determining transition state.

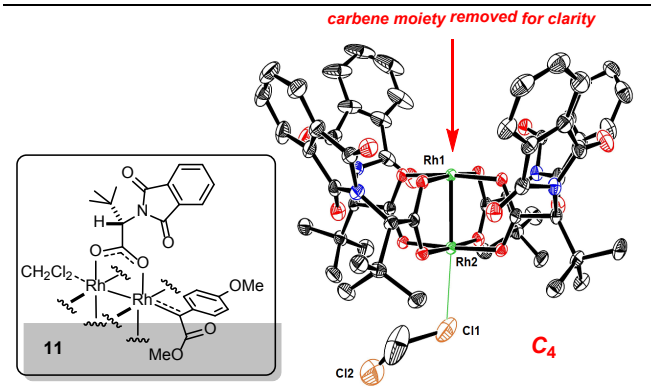

Figure 2. X-ray structure of a chiral dirhodium carbene

Under this premise, it was possible to rationalize the stereochemical course of a cyclopropanation reaction effected by this famous catalyst.[7] Our model predicted the correct isomer; therefore, it also seemed legitimate to analyze why the level of induction is only modest (78% ee). An essentially C_4 symmetric "all up" array entails two notably different rhodium faces (Scheme 6): although the crystallographic data show that the "achiral" pore between the *tert*-butyl groups is narrower than the aperture of the "chiral" calyx, it remains large enough that CH_2Cl_2 can enter and coordinate to Rh2. If a diazo derivative reaches Rh2 and gets decomposed to the corre-

sponding metal carbene, a racemic background reaction will ensue and the *ee* of the resulting product necessarily drops.[7]

Scheme 6. Concept for an Improved Catalyst Design

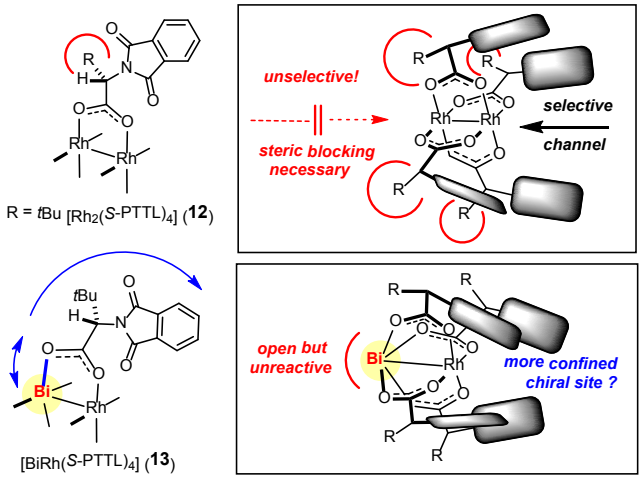

Replacement of the *tert*-butyl groups by even bulkier substituents should improve the outcome; earlier empirical catalyst optimization has shown that this is indeed the case. We pursued a less conventional approach to catalyst optimization, which builds upon recent insights into structure and bonding in heterobimetallic paddlewheel carbene complexes.[8] In a collaboration with the Neese group, we had shown that formal replacement of one Rh^{II} center of the bimetallic core for Bi^{II} enhances the electrophilic character of the resulting carbenes to a significant extent, although the rate of metal-carbene formation is manifestly slower.[9] More important in the present context is the fact that the Bi site lacks any notable Lewis acidity and proved incapable of decomposing ethyl diazoacetate. Even though the ionic radius of Bi is larger than that of Rh and the Bi center hence certainly more exposed, any deleterious background reaction should cease (Scheme 6). Furthermore, the different radii impart a conical shape on the heterobimetallic core, which likely translates into a narrower chiral pocket and hence potentially improves the level of asymmetric induction. As these factors might synergize, it seemed worthwhile to pursue this design concept.[8]

In line with our expectations, the structure of the heterobimetallic analogue [BiRh((*S*)-PTTL)$_4$]·EtOAc (**13**·EtOAc) in the solid state shows that the co-crystallized EtOAc is bound to rhodium, whereas the bismuth center is unligated (Figure 3). Once again, the ligand sphere adopts the α,α,α,α-conformation, presumably because this arrangement places the *tert*-butyl groups as the most bulky substituents at maximum distance from each other; their orientation toward the Bi center follows from the larger radius of this ion, which provides more space. The long Bi–O bonds render the chiral pocket about the rhodium center in **13** more confined than that of its homobimetallic analogue **12**.

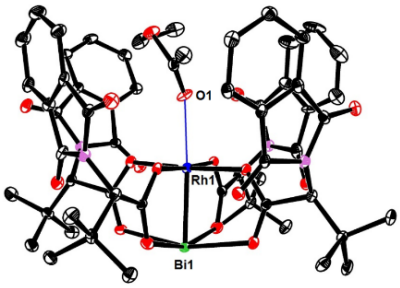

Figure 3. X-ray Structure of [BiRh((*S*)-PTTL)$_4$]·EtOAc

Scheme 7. Superior Performance of the Heterobimetallic Precatalyst 13

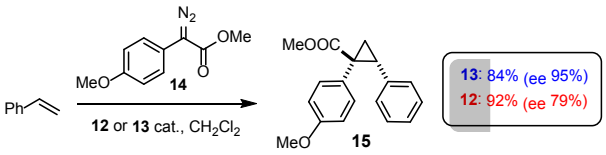

Importantly, the new precatalyst **13** leads to cyclopropanes with notably higher optical purity than those obtained with the traditional dirhodium congener **12** (Scheme 7).[8] This lead finding is the basis for ongoing work in our laboratory which intends to explore the new design and its synthetic implications in more detail.

REFERENCES

(1) Fürstner, A. *J. Am. Chem.Soc.* **2019**, *141*, 11.

(2) Guthertz, A.; Leutzsch, M.; Wolf, L. M.; Gupta, P.; Rummelt, S. M.; Goddard, R.; Farès, C.; Thiel, W.; Fürstner, A. *J. Am. Chem. Soc.* **2018**, *140*, 3156

(3) Biberger, T.; Gordon, C.; Leutzsch, M.; Peil, S.; Guthertz, A.; Copéret, C.; Fürstner, A. *Angew. Chem. Int. Ed.* **2019**, *58*, 8845.

(4) Peil, S.; Guthertz, A.; Biberger, T.; Fürstner, A. *Angew. Chem. Int. Ed.* **2019**, *58*, 8851.

(5) Roşca, D.-A.; Radkowski, K.; Wolf, L. M.; Wagh, M.; Goddard, R.; Thiel, W.; Fürstner, A. *J. Am. Chem. Soc.* **2017**, *139*, 2443.

(6) Meng, Z.; Fürstner, A. *J. Am. Chem.Soc.* **2019**, *141*, 805.

(7) Werlé, C.; Goddard, R.; Philipps, P.; Farès, C.; Fürstner, A. *Angew. Chem. Int. Ed.* **2016**, *55*, 10760.

(8) Collins, L. R.; Auris, S.; Goddard, R.; Fürstner, A. *Angew. Chem. Int. Ed.* **2019**, *58*, 3557.

(9) Collins, L. R.; van Gastel, M.; Neese, F.; Fürstner, A. *J. Am. Chem. Soc.* **2018**, *140*, 13042.